Inorganica Chimica Acta 361 (2008) 3951–3956

Contents lists available at ScienceDirect

Inorganica Chimica Acta

journal homepage: www.elsevier.com/locate/ica

Magnetic behaviour of Mn_{12} single-molecule magnet nanospheres

C. Carbonera [a], I. Imaz [b], D. Maspoch [b], D. Ruiz-Molina [c], F. Luis [a,*]

[a] Instituto de Ciencia de Materiales de Aragón, CSIC-Dpto. de Física de la Materia Condensada Universidad de Zaragoza, 50009 Zaragoza, Spain
[b] Institut Català de Nanotecnologia, Campus UAB-Edifici CM7, 08193 Bellaterra, Spain
[c] Centro de Investigación en Nanociencia y Nanotecnología (CIN2-CSIC), Campus UAB-Edifici CM7, 08193 Bellaterra, Spain

ARTICLE INFO

Article history:
Received 12 February 2008
Received in revised form 5 March 2008
Accepted 10 March 2008
Available online 15 March 2008

Dedicated to Dante Gatteschi.

Keywords:
Single-molecule magnets
Magnetic properties
Mn_{12} acetate
Nanomagnetism

ABSTRACT

Sub-50 nm spherical particles that exhibit single-molecule magnet (SMM) behaviour have been fabricated by direct precipitation of $[Mn_{12}O_{12}(CH_3COO)_{16}(H_2O)_4]$ clusters in a mixture of acetonitrile and toluene. The magnetic properties clearly indicate that particle formation does not affect the molecular composition of $Mn_{12}O_{12}$ clusters, although some interesting differences appear when the magnetic behaviour exhibited by such nanoparticles is compared with a polycrystalline sample of $[Mn_{12}O_{12}(CH_3COO)_{16}(H_2O)_4]$.

1. Introduction

Single-molecule magnets (SMMs), such as Mn_{12}- [1] or Fe_8-based clusters [2] and bis(phthalocyaninato) complexes [3], attract widespread attention for their potential technological applications in high-density information storage molecular devices, spintronic systems, and quantum-computing applications [4]. In such a context, one of the current challenges in the field of SMMs is their processing and structuration either in the form of micro- and nanoparticles or on surfaces [5–7]. In the latter case, nanostructuration of SMMs on different substrates, from gold to polymeric substrates, by using different self-assembly and/or patterned-assisted techniques have been developed [5,6]. The interest is twofold. First, the development of nanostructured motives that are the basis for future molecular devices. And second, obtaining a better knowledge of their SMM behaviour on the transition from the macroscopic to the nanoscopic world. From a physical point of view, it is also interesting to control parameters such as particle size and environmental effects, and to study how they can affect the magnetic relaxation and quantum tunnelling [8]. Thus far, some advances have been done in studying SMMs in different environments. For example, SMMs have been incorporated into porous silica [8b], polymeric matrices [8c] and Langmuir Blodgett films [8d]. In its turn, this fundamental knowledge can prove useful in order to control the behaviour of these clusters when we try to build useful devices for quantum computation and data storage since the degree of decoherence as well as the lifetime of the data stored strongly depend on the magnetic relaxation.

Concerning environmental effects, in the last seven years, it has become evident that disorder plays a non-negligible role in determining the tunnelling rates and the energy splittings between magnetic energy levels. Essentially, two sources of disorder have been considered. First, the disorder that arises from lattice defects such as dislocations [9]. And second, the disorder induced by the local orientation of interstitial molecules from the crystallization process [10]. For the acetate derivative of Mn_{12} cluster (Mn_{12}–Ac) $[Mn_{12}O_{12}(CH_3COO)_{16}(H_2O)_4]$ [11], four acetic acid molecules surrounding the molecular core are equally distributed between 2 equivalent orientations. Depending on their orientation, they establish strong hydrogen bonds to either of the two molecules in the unit cell that distort the local symmetry of the molecule, giving rise to a non-zero orthorhombic transverse term not allowed by the pure tetragonal symmetry of the molecular core. The latter scenario, which would lead to a discrete distribution of the transverse terms in contrast with the continuous distribution expected for lattice defects, agrees better with recent experimental evidences obtained from magnetic relaxation and electronic spin resonance experiments [12].

The motivation of the present work is to investigate the effect of particle size, crystal disorder and defects on the tunnelling rates. In order to perform this type of investigations, Mn_{12}–Ac is considered as an ideal system due to the possibility to fabricate a wide diversity of materials with different dimensions and morphologies. Because of the integrity of these clusters is not affected in the fabrication process, the study of these materials allows very useful

* Corresponding author.
E-mail address: fluis@unizar.es (F. Luis).

0020-1693/$ - see front matter © 2008 Elsevier B.V. All rights reserved.
doi:10.1016/j.ica.2008.03.037

comparisons among different kinds of environments. For instance, micro- and sub-micro particles of complex Mn_{12}–Ac with controlled size and polymorphism have been prepared by dense-gas crystallization techniques, showing a remarkable particle size influence on the magnetization relaxation rates [7b]. With this aim, the focus of the present study is a careful investigation of the magnetic relaxation of Mn_{12}–Ac clusters structured in the form of amorphous sub-50 nm nanospheres [13]. The very broad time window (spanning more than seven decades) covered by ac-susceptibility and magnetization experiments enables us to give a satisfactory description of the relaxation process over a quite large range of temperatures, and to describe and characterize two different tunnelling regions: one below and the other above 3 K.

2. Experimental

2.1. Nanoparticle preparation and characterization

The preparation and characterization of Mn_{12}-based nanospheres were previously described in the literature [13]. Briefly, a macroscopic crystalline sample of $[Mn_{12}O_{12}(CH_3COO)_{16}(H_2O)_4] \cdot 2CH_3COOH \cdot 4H_2O$ (Mn_{12}–Ac) dissolved in acetonitrile was added to an aliquot of toluene under vigorous stirring at room temperature. The mixture was then stirred for 1 h. The resulting Mn_{12}–Ac-based nanoparticles were collected by centrifugation and washed with acetonitrile and toluene. The shape and dimensions of the resulting particles were characterized by field emission scanning electron microscopy (FE-SEM), dynamic light scattering (DLS) and transmission electron microscopy (TEM). Fig. 1 shows a representative TEM image of such Mn_{12}–Ac-based spherical nanospheres, which show an average size of 30 ± 7 nm in diameter.

2.2. Magnetic measurements

Magnetic properties were collected on a powder sample, using the Reciprocating Sample Option (RSO) of a commercial SQUID magnetometer. Unlike dc measurements, where the sample is moved through the coils in discrete steps, the RSO measurements were performed using a servo motor, which rapidly oscillates the sample. These measurements have a sensitivity of 5×10^{-9} emu.

The sample was characterized by measuring the ac-susceptibility as a function of the frequency (between 0.1 Hz and 1.4 kHz) and the temperature (1.8 K < T < 15 K), by measuring dc-susceptibility (χ_{dc}) as a function of the applied magnetic field at selected temperatures, and by performing magnetization relaxation experiments. For the latter study, the spontaneous evolution of the magnetization was followed at a certain temperature during time scales up to 10^4 s. More in detail, while applying an external magnetic field of 10 Oe, the sample was cooled from 10 K to the temperature at which the relaxation was measured. Once stabilized at the desired temperature, the field was turned off, and the measurement was started. In all cases, the sample was mixed with grease (vacuum grease APIEZON N) to prevent grain re-orientation under the action of the external magnetic field. The contributions of the grease and of the sample holder were measured separately and subtracted from the data. These contributions, however, were negligible with respect to that of the sample.

3. Results and discussion

3.1. Equilibrium

Frequency-dependent susceptibility data measured for frequencies $\nu = \omega/2\pi$ between 0.1 Hz and 1.4 kHz are plotted in Fig. 2. Both figures show the typical superparamagnetic freezing associated

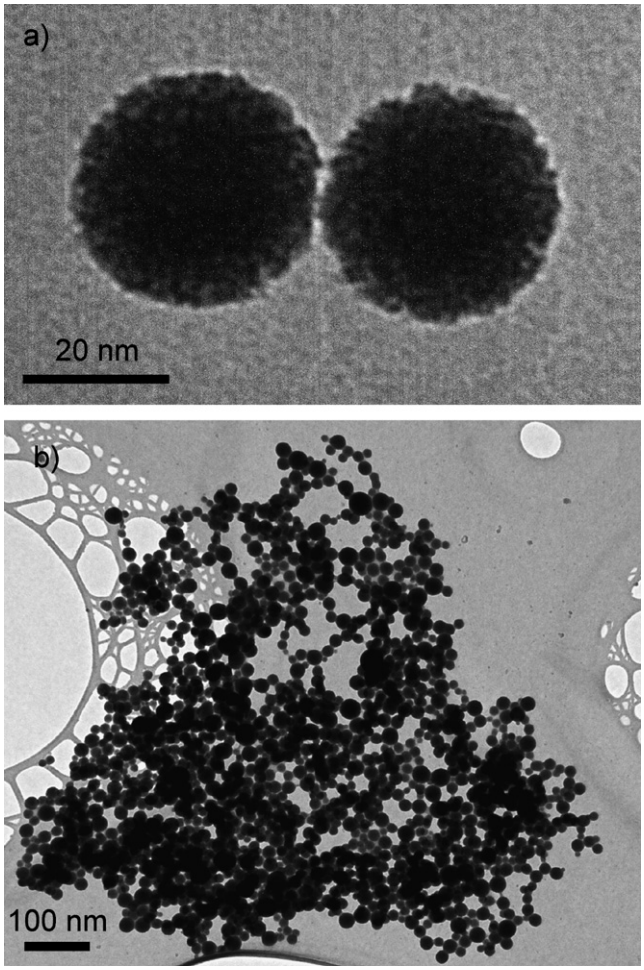

Fig. 1. (a) High-magnification and (b) lower-magnification TEM images of spherical Mn_{12}–Ac-based nanospheres.

with the slow relaxation of SMMs, which takes place below the blocking temperature T_b of the real-part χ'. This blocking temperature decreases with ω. Below T_b, χ' decreases, and this decrease is accompanied by the onset of a non-zero χ''. Above T_b, χ' attains its equilibrium value χ_{eq}. For a powdered sample and in the limit of strong anisotropy (valid in this case), χ_{eq} should follow a Curie–Weiss law; as indeed does for the nanoparticles (Fig. 2, inset). The best fit (solid line in Fig. 2, inset) to the Curie–Weiss equation with $S = 10$ gives $g = 2.04$, which is compatible with clusters having the same ground state as the crystalline Mn_{12} compounds. Moreover, the resulting Weiss temperature ($\theta \approx -0.4$ K) indicates the presence of antiferromagnetic intermolecular interactions. By comparison with the θ value of a polycrystalline sample of Mn_{12}–Ac ($\theta \approx 0.5(1)$ K) [14], we may conclude that both the strength as well as the sign of these interactions are modified by the structural and morphological changes associated with the formation of amorphous nanospheres.

3.2. Hysteresis

Fig. 3 shows the magnetic hysteresis loop for the powdered sample recorded at temperatures of 2 K and 2.3 K, together with the respective derivative curves, showing the presence of resonant quantum tunnelling of the magnetic moment (each peak corresponds to a faster relaxation). It is evident how the hysteresis loop becomes narrower with increasing temperature (to disappear above $T_b \approx 3$ K). The derivative shows peaks centred near $H_0 = 0$ Oe and $H_1 \approx 3.9$ kOe. Also, at higher H values, there is a wide